PHYSICAL REVIEW A VOLUME 23, NUMBER 3 MARCH 1981

Delay-time statistics of superfluorescent pulses

Fritz Haake, Joseph W. Haus, Harald King, and Guntram Schröder
Fachbereich Physik, Gesamthochschule Essen, 4300 Essen, Deutschland

Roy Glauber
Lyman Laboratory of Physics, Harvard University, Cambridge, Massachusetts 02138
(Received 30 July 1980)

We discuss the delay-time statistics of superfluorescent pulses by introducing the concept of a passage time at which the field intensity reaches a specified value. Such passage times can be estimated accurately from the early-stage linear dynamics of the radiating system. The distribution function for the passage times, we show, can be expressed as a functional integral over the random zero point fluctuations of the atomic polarization. The functional integral can be evaluated exactly and reduced to an elementary closed form. Our theory applies both to the sharp and the broadened atomic line. The results we obtain agree with experimental data and numerical calculations already in existence for the unbroadened line. For the broadened line we predict substantial changes of the mean value and the variance of the passage time as the width of the atomic line increases. We also investigate the influence of the shape of the spectral distribution of atomic frequencies and show that the delay statistics depend significantly on the way in which the spectral density decreases in the wings of the atomic line.

I. INTRODUCTION

Superfluorescent pulses are brief intense pulses radiated collectively by groups of many inverted atoms. From a macroscopic point of view, the initial atomic state of complete inversion is a state of unstable equilibrium. Its decay is induced by the presence of microscopic fluctuations in the form of quantum uncertainties of the initial atomic dipole moments.

The radiation process which begins with spontaneous emission proceeds coherently and rapidly amplifies the fields to classically describable magnitudes. The classical description, in fact, begins to hold as soon as the atoms have left the fluctuation-dominated neighborhood of their initial state. To say that the pulse develops classically, however, is not to say that it is predictable. Since the initiation of each pulse is an intrinsically random process, pulses differ significantly in shape from one another.

Among the quantities which display strong pulse-to-pulse fluctuations, the delay time of the pulse maximum is of particular interest since its statistical properties have been measured recently by Vrehen.[1] We have in a previous work,[2] hereafter referred to as I, calculated by numerical means the delay time statistics for a monochromatic atomic line. The agreement with the experiments of Vrehen was found to be satisfactory.

In the present paper we shall show that the delay statistics can be calculated analytically,[3] and that the effects of line broadening can readily be included as well. The results obtained with the present method agree, for the case of the monochromatic line, with both the numerical calculations and the experimental data noted earlier. For the case of the broadened line, on the other hand, we obtain a number of new results. We show, for example, how the mean value and the variance of the delay time change when the width of the atomic line is increased below the mean delay time pertinent to the sharp atomic line, the temporal development of the mean intensity is quite different for the Gaussian line shape than for the Lorentzian one.

Our approach, as in our previous work, describes the atomic polarization and inversion in terms of quantum fields. We present in Sec. II the equations of motion for these fields and for the radiation field We then develop in Sec. III a description of pulse delays by means of appropriately defined passage times. We define and calculate a probability distribution for these passage times which is based on the early-stage linearized dynamics of the system.[4-7] We solve the linearized field equations in Sec. IV. Section V is devoted to the discussion of the way in which the radiated intensity depends upon the shape of the atomic spectral line. In Secs. VI and VII we present the detailed passage time statistics for the monochromatic and the broadened atomic spectral lines.

As a brief characterization of our work and some of its limitations, we would like to add the following remarks. Our quantitative analysis will be made for two-level atoms in a one-dimensional model. We shall use a slowly varying envelope approximation for all fields involved, thus requiring the system to be much longer than a wavelength of the radiation emitted. We shall not include the effects of the pump pulse dynamics, but rather assume complete atomic inversion as an initial condition.

II. EQUATIONS OF MOTION

Let us consider N two-level atoms and describe them by means of the raising operators s_μ^+ with $\mu=1,2,\ldots,N$; the lowering operators s_μ^-; and the "inversion" operators s_μ^z. These operators obey the angular momentum commutation relations

$$[s_\mu^+, s_\nu^-]=\delta_{\mu\nu}2s_\mu^z, \quad [s_\mu^z, s_\nu^\pm]=\pm\delta_{\mu\nu}s_\mu^\pm . \tag{2.1}$$

We will assume the atoms to be identical save for the separation of the two levels. If we denote that separation by $\hbar\omega_\mu$, we may write the Hamiltonian of the noninteracting atoms in the form

$$H_A=\sum_\mu \hbar\omega_\mu s_\mu^z . \tag{2.2}$$

For the sake of simplicity, we take the atomic transition to be one that gives rise to light linearly polarized in the z direction. The transition can then be characterized by a single dipole matrix element which we denote by $\hbar g$. The radiated light can be represented by the z component of the transverse electric field operator at the point $\vec{\mathbf{x}}$, $E_z(\vec{\mathbf{x}})\equiv E(\vec{\mathbf{x}})$. We then write the interaction Hamiltonian in the form

$$H_{AF}=\sum_\mu E(\vec{\mathbf{x}}_\mu)i\hbar g(s_\mu^- - s_\mu^+) . \tag{2.3}$$

From the Hamiltonians H_A and H_{AF} and the well-known free-field Hamiltonian,[8] we find the Heisenberg equations of motion for the operators $s_\mu^{\pm,z}$

$$\dot{s}_\mu^\pm(t)=\pm i\omega_\mu s_\mu^\pm(t)+2gE(\vec{\mathbf{x}}_\mu,t)s_\mu^z(t) , \tag{2.4}$$

$$\dot{s}_\mu^z(t)=-gE(\vec{\mathbf{x}}_\mu,t)[s_\mu^+(t)+s_\mu^-(t)] , \tag{2.5}$$

and the wave equation for the electric field

$$\left(\nabla^2-\frac{1}{c^2}\frac{\partial^2}{\partial t^2}\right)E(\vec{\mathbf{x}},t)=-4\pi\nabla^2P^{\mathrm{Tr}}(\vec{\mathbf{x}},t) . \tag{2.6}$$

The driving term in this inhomogeneous wave equation is provided by the transverse part of the atomic polarization,

$$P^{\mathrm{Tr}}(\vec{\mathbf{x}},t)=i\hbar g\sum_\mu \delta_{zz}^{3\mathrm{Tr}}(\vec{\mathbf{x}}-\vec{\mathbf{x}}_\mu)[s_\mu^-(t)-s_\mu^+(t)] . \tag{2.7}$$

Here $\delta_{zz}^{3\mathrm{Tr}}(\vec{\mathbf{x}})$ denotes the zz component of the transverse δ function

$$\delta_{ij}^{3\mathrm{Tr}}(\mathbf{x})=\int\frac{d^3k}{(2\pi)^3}\left(\delta_{ij}-\frac{k_ik_j}{\vec{\mathbf{k}}^2}\right)e^{i\vec{\mathbf{k}}\cdot\vec{\mathbf{x}}} . \tag{2.8}$$

The above equations of motion describe a dynamical problem in three spatial dimensions. In order to gain insight into the statistical properties of the radiated light, we replace this problem with the much simpler one obtained by restricting the number of spatial dimensions to one. We have argued in I that such a simplification, although drastically idealized, may not be inappropriate if the atoms are confined to a pencil-shaped cylinder with a Fresnel number near unity. We shall think of the cylinder as oriented along the x axis and denote its length and diameter by l and d, respectively. The condition on the Fresnel number then reads $F=d^2/\lambda l\approx 1$.

As a second, much less critical simplification, we require that the number density of atoms, n, be so large that there are many atoms in every transverse section of the cylinder extending over a typical wavelength $\lambda=2\pi(c/\omega)$ along the axis. We may then describe the atoms by means of polarization and inversion densities. In order to define such densities, we think of the cylinder as sliced in transverse sections with a longitudinal extent $\Delta x\ll\lambda$ and label the sections by their x coordinate. Similarly, we introduce frequency intervals $\Delta\nu$, each of which is small compared to the width $1/T_2^*$ of the distribution of the atomic frequencies. By summing the atomic operators $s_\mu^{\pm,z}$ of all atoms within a "cell" $\Delta x\Delta\nu$ at x,ν we obtain the densities

$$J_\alpha(x,t,\nu)=\frac{1}{\Delta V\Delta\nu}\sum_{\substack{\vec{\mathbf{x}}_\mu\in\Delta V\\ \omega_\mu\in\Delta\nu}} s_\mu^\alpha(t), \quad \alpha=+,-,\text{ or } z , \tag{2.9}$$

where $\Delta V=\Delta x\pi d^2/4$ is the volume of a cylinder section.

Analogously, we can describe the electric field by the smoothed-out field operator

$$E(x,t)=\frac{1}{\Delta V}\int_{\Delta V} d^3x E(\vec{\mathbf{x}},t) . \tag{2.10}$$

Although we have defined the fields $J_\alpha(\mathrm{x},t,\nu)$ and $E(x,t)$ in Eqs. (2.9) and (2.10) to depend on a discrete spatial variable and a discrete frequency, we shall, in the following, assume these functions to vary smoothly and adopt the point of view of a macroscopic continuum theory with x and ν as continuous variables.

We easily obtain the equations of motion for the macroscopic fields $J_\alpha(x,t,\nu)$ and $E(x,t)$ from the microscopic equations (2.4)–(2.6). We should note that for the geometry we have chosen we may replace the transverse δ function $\delta_{zz}^{3\mathrm{Tr}}(\vec{\mathbf{x}})$ appearing in (2.7) with the ordinary δ function $\delta^3(\vec{\mathbf{x}})$ since the relevant wave vectors all point in the x direction. The macroscopic field equations then take the form

$$\dot{J}_\pm(x,t,\nu)=\pm i\nu J_\pm(x,t,\nu)+2gE(x,t)J_z(x,t,\nu) , \tag{2.11}$$

$$\dot{J}_z(x,t,\nu)=-gE(x,t)[J_-(x,t,\nu)+J_+(x,t,\nu)] , \tag{2.12}$$

$$\left(\frac{\partial^2}{\partial x^2}-\frac{1}{c^2}\frac{\partial^2}{\partial t^2}\right)E(x,t) =-4\pi\frac{\partial^2}{\partial x^2}i\hbar g\int d\nu[J_-(x,\nu,t)-J_+(x,\nu,t)] . \tag{2.13}$$

Finally, we assume a distribution $W(\nu)$ of the atomic frequencies, which is relatively sharp, i.e., has a width $1/T_2^*$ small in comparison with its center frequency ω. The polarization densities $J_\pm$ and the electric field can then be thought of as slowly modulated plane waves propagating to the right and to the left along the x axis.

We shall define the slowly varying amplitudes or envelope operators for these waves as dimensionless functions of dimensionless variables. To that end, we use the length l of the cylinder as a unit of length and the superfluorescence time τ, which is defined by

$$1/\tau = 2\pi g^2 \hbar n \omega l/c \tag{2.14}$$

as a unit of time. We then represent the atomic fields as

$$J_z(x,t,\nu) = \tfrac{1}{2} n W(\nu) Z\left(\frac{x}{l}, \frac{t}{\tau}, (\nu-\omega)\tau\right), \tag{2.15}$$

$$J_\pm(x,t,\nu) = \tfrac{1}{2} n W(\nu)\left[e^{\mp i(kx-\omega t)} R_\pm\left(\frac{x}{l}, \frac{t}{\tau}, (\nu-\omega)\tau\right) + e^{\pm i(kx+\omega t)} L_\pm\left(\frac{x}{l}, \frac{t}{\tau}, (\nu-\omega)\tau\right)\right];$$

here $k=\omega/c$ is the wave number corresponding to the center frequency of the distribution $W(\nu)$. Similarly, we write for the positive and negative frequency parts of the electric field

$$E^\pm(x,t) = \frac{1}{2g\tau}\left[e^{\pm i(kx-\omega t)} E_R^\pm\left(\frac{x}{l}, \frac{t}{\tau}\right) + e^{\mp i(kx+\omega t)} E_L^\pm\left(\frac{x}{l}, \frac{t}{\tau}\right)\right]. \tag{2.16}$$

By inserting the representations (2.15) and (2.16) into the field equations (2.11)–(2.13) and neglecting rapidly oscillating terms, we obtain the Maxwell-Bloch equations for the slowly varying envelope operators $R_\pm$, $L_\pm$, and $E^\pm_{R,L}$:

$$\dot{R}_\pm(x,t,\nu) = \pm i\nu R_\pm(x,t,\nu) + E_R^\mp(x,t) Z(x,t,\nu),$$
$$\dot{L}_\pm = \pm i\nu L_\pm + E_L^\mp Z,$$
$$\dot{Z} = -\tfrac{1}{2}(E_R^+ R_+ + E_L^+ L_+ + \text{H.c.}),$$
$$\left(\frac{\partial}{\partial x} + \frac{1}{v}\frac{\partial}{\partial t}\right) E_R^\mp(x,t) = \int d\nu\, p(\nu) R_\pm(x,t,\nu),$$
$$\left(-\frac{\partial}{\partial x} + \frac{1}{v}\frac{\partial}{\partial t}\right) E_L^\mp(x,t) = \int d\nu\, p(\nu) L_\pm(x,t,\nu). \tag{2.17}$$

Here, in contrast to Eqs. (2.11)–(2.13), the quantity ν measures the detuning from the center frequency ω, $p(\nu)$ is a dimensionless form of the frequency distribution

$$p(\nu) = \frac{1}{\tau} W\left(\frac{\omega+\nu}{\tau}\right), \tag{2.18}$$

and v is the dimensionless expression for the velocity of light,

$$v = c\tau/l. \tag{2.19}$$

The Maxwell-Bloch equations (2.17) generalize the equations treated in I to the case of an inhomogeneously broadened atomic line.

The field equations (2.17) have to be solved with the boundary condition that no external signals impinge on the cylinder at $x=0$ or $x=1$, and with appropriate initial conditions for all the fields at $t=0$. Once we have found the corresponding solutions we can calculate, for example, the nth normally ordered moment of the intensity radiated to the right as the expectation value

$$I^{(n)}(t) = \langle \text{vac}, \{\uparrow\} | E_R^-(1,t)^n E_R^+(1,t)^n | \text{vac}, \{\uparrow\} \rangle, \tag{2.20}$$

where

$$|\text{vac}, \{\uparrow\}\rangle \tag{2.21}$$

denotes the initial state of the system. This initial state is the vacuum of the electromagnetic field and the excited state for each atom; it is an eigenstate of the operator $Z(x,0,\nu)$ with eigenvalue one.

Since the polarization fields R_+ and R_- are the sources for the electric fields E_R^- and E_R^+, respectively, it is convenient, as we have shown in I, to derive the normally ordered moments (2.20) from a standard set of ordered atomic expectation values

$$A_{nm} = \langle \text{vac}, \{\uparrow\} | R_+(x_1,0,\nu_1) \ldots R_+(x_n,0,\nu_n) Z(x_1'',0,\nu_1'') \ldots Z(x_m'',0,\nu_m'') R_-(x_1',0,\nu_1') \ldots R_-(x_n',0,\nu_n') | \text{vac}, \{\uparrow\} \rangle. \tag{2.22}$$

By using the definitions (2.9) and (2.15) we can show, as in I, that the operators Z in (2.22) can be replaced, up to corrections of order $1/N$, by unit operators. The expectation value $A_{nm} = A_{no}$ may then be expressed as a sum of products of two-point expectation values $A_{10}(x_i - x_j', \nu_i, \nu_i')$

$$A_{no} = \sum_P A_{10}(x_1 - x_1', \nu_1, \nu_1') A_{10}(x_2 - x_2', \nu_2, \nu_2') \ldots A_{10}(x_n - x_n', \nu_n, \nu_n'). \tag{2.23}$$

Here the sum runs over all $n!$ permutations of the primed variables. The basic two-point function is given by

$$A_{10}(x-x',\nu,\nu')=\frac{4}{N}\delta(x-x')\delta(\nu-\nu')p(\nu)^{-1}\,. \tag{2.24}$$

The spatial delta function, as we have seen in I, is due to the fact that the expectation value A_{10} contains no contributions from pairs of different atoms, but is instead a sum of single-atom contributions. The delta function $\delta(\nu-\nu')$ has the same origin. The factor $p(\nu)^{-1}$ follows from our normalization condition (2.15).

The results (2.23) and (2.24) can be obtained equivalently by regarding the initial polarization operator $R_+(x,0,\nu)$ as a classical complex random field with the Gaussian probability density

$$P(\{R\})=\mathfrak{N}\exp\left(-\frac{N}{4}\int_0^1 dx\int_{-\infty}^{+\infty}d\nu p(\nu)\,|R_+(x,0,\nu)|^2\right). \tag{2.25}$$

The factor $\mathfrak{N}$ is defined so that the functional integral of $P(\{R\})$ is normalized to unity,

$$1=\int d^2\{R\}P(\{R\})\,. \tag{2.26}$$

As we have shown in I (by using a suitable quasi-probability functional to represent the density operator), each superfluorescent pulse develops classically in the following sense. To within corrections of relative order $1/N$, the fields $R_\pm$, $L_\pm$, Z, and $E^\pm_{R,L}$ can all be treated as c-number fields obeying classical equations of motion of the form (2.17). The quantum nature of the pulses then appears solely in the uncertainty of the initial atomic polarization which is described by the probability distribution (2.25). We shall continue to use this classical probability description in the present paper. To simplify the notation we shall denote by $E(x,t)$ and $R(x,t,\nu)$ the complex random fields associated with the operators $E^-_R(x,t)$ and $R_+(x,t,\nu)$, respectively.

III. THE PASSAGE TIME PROBLEM

We shall next show that the way in which the delay time of the superfluorescent pulses fluctuates can be described by a simple probability distribution. To that end it is convenient to define the delay of a pulse by means of the time t_p at which the pulse intensity at one of the end faces of the cylinder reaches a certain reference intensity I_{ref}.[9] As illustrated in Fig. 1 this passage time is typically somewhat smaller than the delay time t_d of the first maximum of the pulse. However, if the reference intensity is chosen to be of a magnitude comparable to the mean maximum intensity, i.e.,

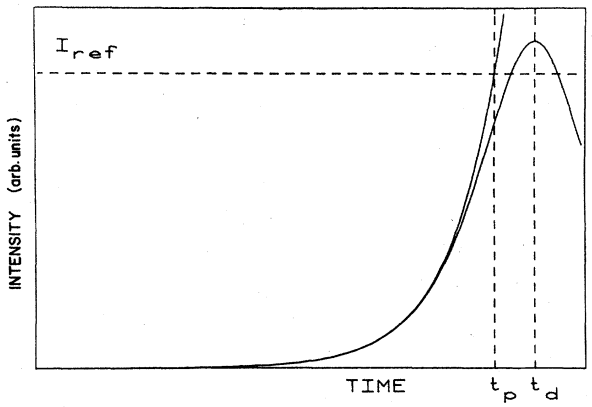

FIG. 1. Definition of the passage time t_p and the delay time t_d. For most trajectories $t_p \approx t_d$.

$$I_{ref}=\mathcal{O}(1)\,, \tag{3.1}$$

the difference between t_p and t_d is relatively small and easily estimated.

The passage time t_p can be much easier to calculate than the delay time t_d. Indeed, superfluorescent pulses tend to rise quite steeply with time to their first intensity maximum. The nonlinearity of the pulse dynamics therefore becomes important only shortly before the first maximum is reached. We can thus estimate the passage time and its statistical properties from the early-stage linear dynamics of the pulse evolution withour appreciable error.

In the early-stage linear regime we can approximate the atomic inversion density as

$$Z(x,t,\nu)=1\,. \tag{3.2}$$

The left- and right-going waves are then decoupled. The passage time for the right-going pulse depends on the random initial polarization $R(x,0,\nu)$,

$$t_p=t_p(\{R\})\,, \tag{3.3}$$

and will thus vary randomly from one pulse to the next. Our task is to relate the probability distribution of t_p to the Gaussian distribution (2.25) of the initial polarization.

As a convenient definition of a passage time distribution, we propose the following functional average over the initial polarization

$$W(t)=\left\langle\delta(|E(t)|^2-I_{ref})\left|\frac{d}{dt}|E(t)|^2\right|\Theta\left(\frac{d}{dt}|E(t)|^2\right)\right\rangle. \tag{3.4}$$

To interpret this definition, we note that the delta function peaks at the passage time, $t=t_p(\{R\})$; the

modulus of the time derivative of the intensity multiplying the delta function effectively turns the latter into a delta function with the argument $t-t_p(\{R\})$; the unit step function in (3.4) serves to reject from the averaging procedure all passages with negative slope, if there are any for a given trajectory.

It follows from the definition (3.4) that the normalization integral $\int_0^\infty dt\, W(t)$ is the mean number of passages of the intensity $|E(t)|^2$ with positive slope per trajectory. Were we to set the reference intensity at values comparable to the mean square of the initial polarization fluctuations, we would have to expect typical trajectories to cross the level I_{ref} more than once; for such small intensities the randomness of the initial polarization configuration can lead to interference effects which cause the radiated intensity to decrease as well as increase. For that reason alone the passage time distribution (3.4) would then have little relation to the delay of the macroscopic pulse. If, however, we set the reference intensity at a macroscopic level as indicated in (3.1), the first passage is likely to occur at a time long compared to a photon transit time l/c. For such times spatial and temporal irregularities of the fields E and R due to the initial irregularity of R have already been washed out and the overwhelming majority of intensity trajectories passes I_{ref} no more than once with positive slope. The excess of the normalization integral $\int_0^\infty dt\, W(t)$ over unity should then be of order no larger than $1/\sqrt{N}$, and thus negligible.

For further discussion and eventual evaluation we express the linear relationship between the electric field at $x=1$ and the initial polarization in the form of an integral,

$$E(t)=\int_0^1 dx\int_{-\infty}^{+\infty} d\nu\, p(\nu)e(x,t,\nu)R(x,0,\nu)\,, \quad (3.5)$$

in which $e(x,t,\nu)$ is a kernel function which we need need not specify until Sec. IV. As a first application of the relation (3.5), we can show that the intensity $|E(x=1,t)|^2$ need not increase monotonically with time.

The time derivative of the intensity is a quadratic form in the initial polarization,

$$\frac{d}{dt}|E(t)|^2=\int_0^1 dx\int_0^1 dx'\int_{-\infty}^{+\infty} d\nu\int_{-\infty}^{+\infty} d\nu' p(\nu)p(\nu')[\dot e(x,t,\nu)e(x',t,\nu')^*+\text{c.c.}]R(x,0,\nu)R(x',0,\nu')^*\,. \quad (3.6)$$

We find two eigenvectors of the "matrix"

$$K(x\nu,x'\nu')=p(\nu)p(\nu')[\dot e(x,t,\nu)e(x',t,\nu')^*+\text{c.c.}]$$

in the form

$$V(x,\nu)=\alpha e(x,t,\nu)+\beta\dot e(x,t,\nu)\,,$$

where the constants α and β are to solved for. The eigenvalues that solve the ensuing quadratic secular equation can be expressed in terms of the average intensity

$$I(t)=\langle|E|^2\rangle=\frac{4}{N}\int_0^1 dx\int_{-\infty}^{+\infty} d\nu\, p(\nu)|e(x,t,\nu)|^2\,, \quad (3.7)$$

the average squared derivative of the electric field

$$\langle|\dot E|^2\rangle=\frac{4}{N}\int_0^1 dx\int_{-\infty}^{+\infty} d\nu\, p(\nu)|\dot e(x,t,\nu)|^2\,, \quad (3.8)$$

and the expectation value

$$\langle\dot E E^*\rangle=\frac{4}{N}\int_0^1 dx\int_{-\infty}^{+\infty} d\nu\, p(\nu)\dot e(x,t,\nu)e(x,t,\nu)^*\,. \quad (3.9)$$

The two eigenvalues we seek for the matrix $K(x\nu,x'\nu')$ then take the form

$$\lambda_\pm=\frac{N}{8}\{\dot I(t)\pm[\dot I(t)^2+4\Delta(t)^2]^{1/2}\}\,, \quad (3.10)$$

in which

$$\Delta(t)^2=\langle|E|^2\rangle\langle|\dot E|\rangle-|\langle\dot E E^*\rangle|^2\,. \quad (3.11)$$

Because of the Schwarz inequality, the function $\Delta(t)^2$ is non-negative. We conclude that one of the eigenvalues (3.10) must be negative, and that the intensity $|E(t,\{R\})|^2$ itself cannot increase monotonically for all initial polarizations.

We now return to the expression (3.4) and perform the functional average over the initial polarization with the weight functional (2.25). That task is simplified by employing the familiar Fourier integral representations for the delta function and the unit step function,

$$\delta(x)=\int_{-\infty}^{+\infty}\frac{d\omega}{2\pi}e^{-i\omega x}\,,$$
$$\Theta(x)=\int_{-\infty}^{+\infty}\frac{d\Omega}{2\pi}\frac{e^{-i\Omega x}}{-i\Omega+\epsilon}\,,\quad \epsilon\to 0^+\,. \quad (3.12)$$

The expression (3.4) then takes the form

$$W(t)=-\int\frac{d\omega}{2\pi}\exp(-i\omega I_{ref})\times\int\frac{d\Omega}{2\pi}\frac{1}{-i\Omega+\epsilon}\frac{\partial}{\partial i\Omega}\times\left\langle\exp\left(-i\omega|E|^2-i\Omega\frac{d}{dt}|E|^2\right)\right\rangle. \quad (3.13)$$

Upon inserting the linear relation (3.5) in (3.13) we see that the remaining functional integral over the initial polarization is Gaussian in nature,

$$\left\langle \exp\left(-i\omega|E|^2 - i\Omega\frac{d}{dt}|E|^2\right)\right\rangle = \mathfrak{N}\int d^2\{R(x,\nu)\}\exp\left(-\int dx\int dx'\int d\nu\int d\nu' M(x\nu,x'\nu')R(x,\nu)R^*(x',\nu')\right),$$

with the matrix

$$M(x\nu,x'\nu') = \frac{N}{4}\delta(x-x')\delta(\nu-\nu')p(\nu) + i\omega p(\nu)p(\nu')e(x,t,\nu)e^*(x',t,\nu') + i\Omega p(\nu)p(\nu')[\dot{e}(x,t,\nu)e^*(x',t,\nu') + e(x,t,\nu)\dot{e}^*(x',t,\nu')]\,. \tag{3.14}$$

We show in the Appendix that the evaluation of this functional integral can be reduced to the calculation of the determinant of a two by two matrix. The result we find is simply

$$\left\langle \exp\left(-i\omega|E|^2 - i\Omega\frac{d}{dt}|E|^2\right)\right\rangle = [1 + i\omega I(t) + i\Omega\dot{I}(t) + \Omega^2\Delta(t)^2]^{-1}\,. \tag{3.16}$$

We now insert Eq. (3.16) in Eq. (3.13) and immediately perform the integral over ω by observing that the integrand has a pole at $\omega = i(1 + i\Omega I + \Omega^2\Delta^2)/I$. The result is

$$W(t) = \frac{1}{I(t)}\int\frac{d\Omega}{2\pi}\frac{1}{\Omega + i\epsilon}\frac{\partial}{\partial\Omega} \times \exp\left(-\frac{I_{\rm ref}}{I(t)}[1 + i\Omega\dot{I}(t) + \Omega^2\Delta(t)^2]\right). \tag{3.17}$$

The remaining integration is elementary and yields the probability distribution for the passage time[10]

$$W(t) = \frac{\dot{I}(t)I_{\rm ref}}{2I(t)^2}e^{-I_{\rm ref}/I(t)}\left(1 + \mathrm{erf}\left[\frac{\dot{I}(t)^2 I_{\rm ref}}{4I(t)\Delta(t)^2}\right]^{1/2}\right) + \left(\frac{[I_{\rm ref}\Delta(t)^2]^{1/2}}{\pi I(t)^3}\right)\exp\left(-\frac{I_{\rm ref}}{I(t)} - \frac{\dot{I}(t)^2 I_{\rm ref}}{4I(t)\Delta(t)^2}\right). \tag{3.18}$$

It should be noted that this result is only based upon the linearity of the relation (3.5). It holds irrespective of the spatial dimensionality of the problem or of the shape of the atomic spectral density $p(\nu)$. While the dimensionality and the shape of the spectral line do affect, of course, the mean intensity $I(t)$ and the averages entering the function $\Delta(t)$, the form of Eq. (3.18) turns out to be quite universal.

IV. EARLY-STAGE SOLUTIONS

The explicit evaluation of the passage time distribution (3.18) requires us to know the kernel function $e(x,t,\nu)$ in the linear relation (3.5). In order to construct it we have to solve the linearized versions of the Maxwell-Bloch equations (2.17), i.e.,

$$\dot{R}(x,t,\nu) = i\nu R(x,\nu t) + E(x,t)\,,$$

$$\left(\frac{\partial}{\partial x} + \frac{1}{v}\frac{\partial}{\partial t}\right)E(x,t) = \int_{-\infty}^{+\infty} d\nu\, p(\nu)R(x,t,\nu)\,. \tag{4.1}$$

We do that by recasting them as equations for the space-time Laplace transforms $R(q,s,\nu)$ and $E(q,s)$, defined, for example, by

$$E(q,s) = \int_0^\infty dx\, e^{-qx}\int_0^\infty dt\, e^{-st}E(x,t)\,. \tag{4.2}$$

By using the boundary and initial conditions $E(x=0,s) = E(q,t=0) = 0$ we then find the transform of the electric field to be

$$E(q,s) = \left(q + \frac{s}{v} - \int_{-\infty}^{+\infty} d\nu\frac{p(\nu)}{s - i\nu}\right)^{-1}R(q,t=0,\nu)\,. \tag{4.3}$$

By inverting the spatial Laplace transform we can write the electric field at the right end of the cylinder in the form

$$E(x=1,s) = \int_0^1 dx\int_{-\infty}^{+\infty} d\nu\, p(\nu)R(x,t=0,\nu)e(x,s,\nu)\,, \tag{4.4}$$

where the kernel function is

$$e(x,s,\nu) = (s - i\nu)^{-1}\exp\{-(1-x)[s/v - \varphi(s)]\}\,, \tag{4.5}$$

$$\varphi(s) = \int_{-\infty}^{+\infty} d\nu\frac{p(\nu)}{(s - i\nu)}\,. \tag{4.6}$$

To proceed further with the inversion we must now specify the spectral distribution $p(\nu)$ of the atomic frequencies. Two distributions which obviously merit consideration are furnished by the Lorentzian and Gaussian line shapes. We have found it interesting to consider a larger family of spectral distributions which interpolate between these as extremes. These distributions can be written as

$$p_n(\nu) = \frac{\mathfrak{N}_n}{[1 + (T\nu)^2/n]^n}\,, \quad n = 1,2,3,\ldots, \tag{4.7}$$

where T is a relaxation time proportional to the dephasing time T_2^* of the atoms, and $\mathfrak{N}_n$ is the normalization factor,

$$\mathfrak{N}_n = \frac{T2^{n-1}(n-1)!}{\pi\sqrt{n}(2n-3)!!}\,. \tag{4.8}$$

The Lorentz line shape then corresponds to $n=1$ while the Gaussian line shape is approached for $n\to\infty$,

$$p_\infty(\nu)=\frac{T}{\sqrt{\pi}}e^{-T^2\nu^2}. \tag{4.9}$$

In the limit $T\to\infty$, all distributions of this family approach the delta function $\delta(\nu)$ which corresponds to a sharp atomic line.

All the distributions (4.7) permit an explicit evaluation of the integral (4.6) by an elementary application of the calculus of residues. The most important special cases are[10]

$$\varphi_1(s)=1/(s+1/T), \tag{4.10}$$

$$\varphi_2(s)=1/(s+\sqrt{2}/T)+(\sqrt{2}/T)/(s+\sqrt{2}/T)^2, \tag{4.11}$$

$$\varphi_\infty(s)=\sqrt{\pi}\,T\exp(T^2s^2)\operatorname{erfc}(Ts). \tag{4.12}$$

In the limit of a sharp atomic line, $T\to\infty$, all $\varphi_n(s)$ approach the function $1/s$.

For small values of the parameter n, it is convenient to reduce the inverse Laplace transform of the function $e(x,s,\nu)$ to sums of convolution integrals of elementary functions. For the Lórentzian line $n=1$, for example, we can write the kernel function $e_1(x,t,\nu)$ as

$$e_1(1-x,t,\nu)=\Theta(t-x/v)e^{-(t-x/v)/T}$$
$$\times\left\{I_0(2[x(t-x/v)]^{1/2})+\int_0^{t-x/v}dt'I_0(2\sqrt{xt'})\left(i\nu+\frac{1}{T}\right)\exp\left[\left(i\nu+\frac{1}{T}\right)\left(t-t'-\frac{x}{v}\right)\right]\right\}, \tag{4.13}$$

where I_0 is the modified Bessel function of order zero.[10] In the next simplest case, $n=2$, the corresponding result is

$$e_2(1-x,t,\nu)=\Theta(t-x/v)\Phi\left(x,t-\frac{x}{v}\right)+\left(i\nu+\frac{\sqrt{2}}{T}\right)\int_0^{t-x/v}dt'\,\Phi(x,t')e^{i\nu(t-t'-x/v)} \tag{4.14}$$

with

$$\Phi(x,t)=e^{-\sqrt{2}t/T}\frac{1}{\pi}\int_0^\pi d\Theta\exp[2\sqrt{tx'}\cos\Theta+(\sqrt{2}t/T)\cos2\Theta]\left(\frac{\sqrt{2t}}{T}\sin2\Theta\right).$$

The integral $\Theta(x,t)$ can also be represented as a sum of Bessel functions,

$$\Theta(x,t)=e^{-(\sqrt{2}t/T)}\sum_{m=0}^{\infty}\frac{1}{m!}\left(\frac{\sqrt{2}t}{T}\right)^m I_{2m}(2\sqrt{xt}). \tag{4.15}$$

For larger values of the index n, the expressions for the kernel $e_n(x,t,\nu)$ rapidly become lengthier. Rather than presenting them, we proceed directly to the Gaussian limit, $n\to\infty$. In that limit it is convenient to write the kernel as

$$e_\infty(1-x,t,\nu)=\Theta(t-x/v)\left[\Psi\left(x,t-\frac{x}{v}\right)+i\nu\int_0^{t-x/v}dt'\Psi(x,t')e^{i\nu(t-t'-x/v)}\right], \tag{4.16}$$

where the function $\Psi(x,t)$ can only be found numerically as the inverse temporal Laplace transform of

$$\Psi(x,s)=\frac{1}{s}e^{-x\varphi_\infty(s)}. \tag{4.17}$$

By inserting the kernels $e(x,t,\nu)$ just calculated in the expressions (3.7), (3.8), and (3.9), we find all the expectation values needed for the evaluation of the passage time distribution (3.18). One feature of these expectation values is perhaps worth mentioning. As a consequence of the slowly varying envelope approximation we have made in Sec. II the kernel $e(x,t,\nu)$ is discontinuous at $t=x/v$. The time derivative $\dot{e}$ has a delta-function singularity at that time. Consequently, the expectation value $\langle|\dot{E}|^2\rangle$ given by Eq. (3.8) diverges until the field discontinuity propagates out of the cylinder, that is, until a transit time $1/v$. In order to calculate $\langle|\dot{E}|^2\rangle$ and the passage time distribution $W(t)$ for times $t\leq 1/v$, we would have to abandon the slowly varying envelope approximation. Fortunately, however, in typical experiments the transit time is smaller than unity (in units of the superfluorescence time), and much smaller still than the mean delay time. For times t which are that small, no significant fraction of the ensemble of trajectories has risen to the macroscopic intensity level $I_{\rm ref}$. No measurable error is thus incurred by simply taking $W(t)$ to vanish for $t\leq 1/v$.

V. THE MEAN RADIATED INTENSITY FOR DIFFERENT ATOMIC LINE SHAPES

If the radiating atoms move freely in space with a thermal velocity distribution, the spectrum of their transition frequencies is Doppler broadened and thus Gaussian in form. However, as we have indicated in Sec. IV, the Gaussian spectrum is a computationally difficult one to treat. Before undertaking this treatment, it is worth investigating the dependence of the pulse statistics on the index n which determines the line shapes $p_n(\nu)$. The simplest quantity we can study in this sense is the average radiated intensity $I(t)$. When we evaluate it from Eq. (3.7) and the kernels $e_n(x,t,\nu)$ appropriate to the spectral distributions $p_n(\nu)$, we must exercise care in choosing the parameter T.

It is natural to define the dephasing time T_2^* of the atomic polarization by identifying it with the parameter $T \equiv T^{(\infty)}$ appearing in the Gaussian distribution (4.9). There is, however, no unique way of relating the parameter $T \equiv T^{(n)}$ which characterizes the width of the distributions (4.7) to the dephasing time $T_2^* = T^{(\infty)}$. A physically sensible definition of $T^{(n)}$, which we shall adopt in the following, is given the requirement that the gain factor of the inverted atomic medium be independent of the index n. Since the gain factor is proportional to $p_n(0)$, we choose as a definition of the parameter $T^{(n)}$

$$p_n(0) = \mathfrak{N}_n = \frac{T^{(n)} 2^{n-1}(n-1)!}{\pi\sqrt{n}(2n-3)!!} = \mathfrak{N}_\infty = \frac{T_2^*}{\sqrt{\pi}}. \qquad (5.1)$$

We show in Fig. 2 two families of mean intensities for $n=1$, 2, 3, and ∞. One of the families corresponds to $T_2^* = 6.75$, the other one to $T_2^* = 47.7$. The parameters $\mathfrak{N}$ and v are the same for all curves and imply a mean delay time of the first pulse maximum $\langle t_d \rangle = 33$ for $T_2^* = \infty$. The interesting inference to be drawn from these curves is that, except for large values of T_2^*, i.e., larger than the mean delay time, the intensities $I(t)$ depend sensitively on the index n. Indeed, the intensities corresponding to the Lorentzian and the Gaussian line differ by as much as an order of magnitude at times comparable to the mean delay time unless the dephasing time is larger than the mean delay time. We conclude, therefore, that a quantitative description of the effect of inhomogeneous line broadening on superfluorescent pulses must be based on the Gaussian line shape.

The broadening of the atomic line has an additional consequence worthy of mention. By causing different components of the polarization to oscillate with different frequencies, it leads to dephasing, a process which eventually competes significantly with the amplification process and tends to cancel it out altogether. In that limit the inhomogeneous term in the second of Eqs. (4.1) goes to zero and the radiated intensity $|E(1,t)|^2$ approaches a constant value. Only in the limit of a sharp atomic line does the amplification continue indefinitely.

This competition of amplification and dephasing is most easily illustrated for the Lorentz line shape. The mean radiated intensity for that case reads

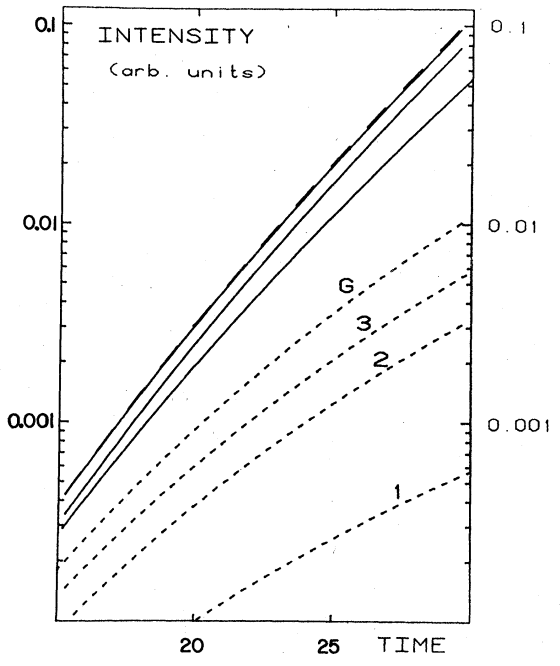

FIG. 2. Mean intensities as functions of time for $T_2^* = 6.75$ (lower four curves) and $T_2^* = 47.7$ (upper four curves). The labels on the lower four curves refer to the index n characterizing the line shape function (4.7); especially, $n=1$ refers to the Lorentzian line while the label G corresponds to the Gaussian line $n=\infty$. The upper four curves correspond to the same sequence of line shape functions. The uppermost one of them which again corresponds to the Gaussian line, is dashed for better visibility; to within the accuracy of the plot this curve coincides with that of the mean intensity for the monochromatic atomic line $T_2^* = \infty$. All curves are evaluated for $N = 1.5\times 10^8$ and $1/v = 0.3$.

$$I(t) = \frac{4}{N}\int_0^1 dx\, \Theta(t - x/v)\left[e^{-2(t-x/v)/T_2^*} I_0(2[x(t-x/v)]^{1/2})^2 + \left(\frac{2}{T_2^*}\right)\int_0^{t-x/v} dt'\, e^{-2t'/T_2^*} I_0(2\sqrt{xt'})^2\right]. \qquad (5.2)$$

While the first term in this expression decays to zero in time, the second approaches the constant value

$$I(\infty)=\frac{8}{NT_2^*}\int_0^\infty dt\, e^{-2t/T_2^*}\int_0^1 dx\, I_0(2\sqrt{xt})^2$$
$$=\frac{8}{NT_2^*}\int_0^\infty dt\, e^{-2t/T_2^*}[I_0(2\sqrt{t})^2-I_1(2\sqrt{t})^2]\,. \tag{5.3}$$

For sufficiently small values of the dephasing time T_2^*, the radiated intensity (5.2) can approach the asymptotic value $I(\infty)$ well within the time interval in which the linear approximation is valid. In that limit, of course, the radiation process is overwhelmed by the dephasing and shows little tendency toward cooperative behavior; radiation emitted in this regime has been called amplified spontaneous emission.[11]

VI. PASSAGE TIME STATISTICS FOR A SHARP ATOMIC LINE

The limiting case of a monochromatic atomic line $T_2^*\to\infty$ deserves special attention because it enables us to compare the passage time statistics calculated in the present paper with the delay time statistics we have calculated previously by numerical means.[2] By taking the limit $T\to\infty$ in Eq. (4.13) we find that the kernel reduces to the well-known form[2,5,12]

$$e(x,t)=\Theta(t-x/v)I_0(2[x(t-x/v)]^{1/2})\,. \tag{6.1}$$

If we use this expression to calculate the expectation values $I(t)$ and $\Delta(t)$ we find the passage time probability distribution which is plotted as the solid curve in Fig. 3. The histogram in that figure is the numerical result for the probability distribution of the delay time of the first pulse maximum.[2] The passage time distribution $W(t)$ shown corresponds to a value of the reference intensity $I_{\rm ref}$ chosen so that the most probable delay time coincides with the most probable passage time. The agreement of the two distribution functions substantiates the physical arguments given in Sec. III.

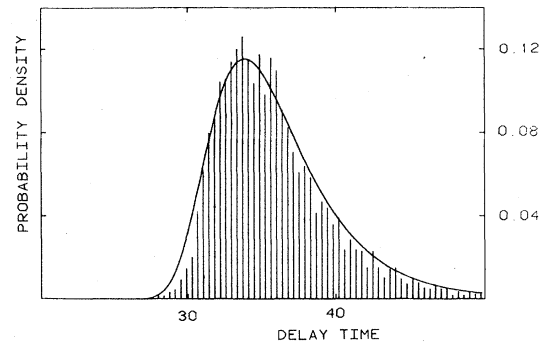

FIG. 3. The histogram shows the distribution of the delay time t_d obtained from a large number of numerical solutions of the nonlinear Maxwell-Bloch equations as described in Ref. 2. The solid curve is the passage time distribution $W(t)$ (3.18) with the reference intensity chosen so that the maxima of $W(t)$ and of the histogram occur simultaneously, $I_{\rm ref}=0.43$. All calculations were done for $N=1.5\times10^8$, $1/v=0.3$, $T_2^*=\infty$.

Vrehen has recently measured the delay time statistics for superfluorescent pulses radiated by a pair of independent identically excited cylinders of Cs atoms. His experiment measures the difference of the two delay times. Figure 4 shows the experimental histogram for the delay time difference. The solid curve in Fig. 4 represents the function

$$P(t)=\int_{1/2|t|}^\infty d\tau\, W\left(\tau+\frac{t}{2}\right)W\left(\tau-\frac{t}{2}\right) \tag{6.2}$$

as evaluated from our present result (3.18) for the passage time distribution $W(t)$. The value of $I_{\rm ref}$ chosen here is the same as the one used to calculate the distribution $W(t)$ shown in Fig. 3. The agreement of the theoretical curve with the experimental histogram is evidently close.[13]

VII. PASSAGE TIME DISTRIBUTION FOR BROADENED LINES

We found in Sec. V that the Lorentz line shape $p_1(\nu)$ yields results for the radiated intensity which differ significantly from those of the more realistic Gaussian line shape $p_\infty(\nu)$. When we turn to a discussion of the passage time statistics the Lorentzian line shape becomes even less useful. Indeed, if we calculate the mean values $\langle|E(t)|^2\rangle$ from Eqs. (3.8) and (4.13) we find it to contain

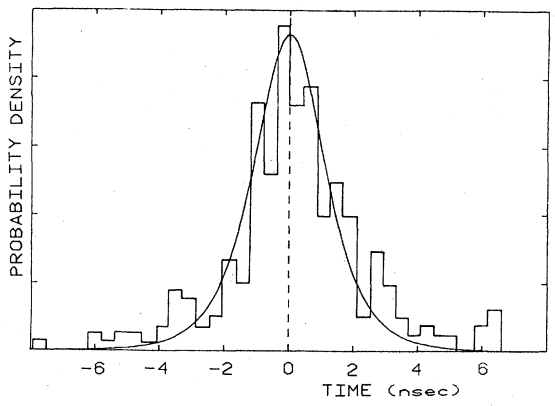

FIG. 4. The experimental delay time histogram of Vrehen (Ref. 1) versus our result (6.2) for $N=1.5\times10^8$, $1/v=0.3$, $T_2^*=\infty$.

an additive term of the form

$$\frac{4}{N}\int_0^1 dx \int_{-\infty}^{+\infty} d\nu\, p_1(\nu)\{I_0(2[x(t-x/v)]^{1/2}\}^2\left(\frac{1}{T^2}+\nu^2\right). \tag{7.1}$$

The frequency integral in this expression diverges since the Lorentz distribution $p_1(\nu)$ has no second moment.

No such difficulty arises for any other of the frequency distributions $p_n(\nu)$ introduced in Sec. IV. We display in Figs. 5 and 6 families of passage time distributions $W(t)$ for various values of the dephasing time T_2^*. These figures serve to compare the distributions for the spectral density $p_2(\nu)$ with those corresponding to the Gaussian density $p_\infty(\nu)$. We conclude from them that the mean passage time begins to increase significantly as the dephasing time T_2^* is made smaller than the mean passage time characteristic of the sharp line. This increase expresses the fact that the dephasing of the atomic dipoles tends to impede the cooperative buildup of the radiation pulse.[14]

It should also be noted in Figs. 5 and 6 that, for a fixed value of the dephasing time T_2^*, the Gaussian spectrum leads, on the average, to smaller passage times than the spectrum $p_2(\nu)$. That is so since the Gaussian distribution has less weight in its wings than the distribution $p_2(\nu)$ and thus resembles the sharp atomic line more closely. A close inspection of Figs. 5 and 6 reveals that as T_2^* is decreased, the variance of the passage time grows somewhat more rapidly than the mean passage time itself.

We have checked the passage time distribution as calculated from Eq. (3.18) against the distribution of first passage times obtained from a large number of numerical solutions of the nonlinear Maxwell-Bloch equations (2.17). In calculating the nonlinear trajectories we have represented the broadened atomic line by five different frequencies and have partitioned the total number of atoms between them according to the Gaussian distribution $p_\infty(\nu)$. Even though such a representation of the broadened line is a rather rough one, we find, for reference intensities I_{ref} within the linear domain, excellent agreement between the histograms obtained numerically and the corresponding distributions $W(t)$. In fact, for a reference intensity I_{ref} as large as 50% of the maximum of the mean radiated intensity the linear theory presented in the present paper gives, quite satisfactory results, as can be seen from Fig. 7. The various curves

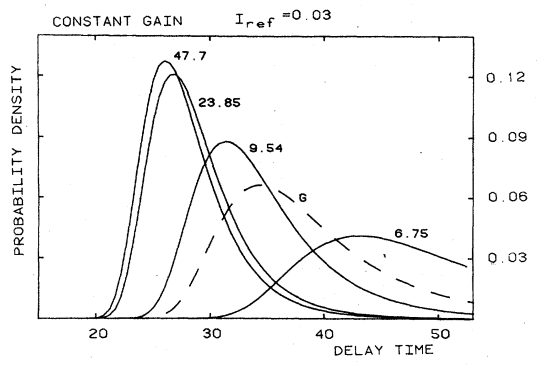

FIG. 5. The solid curves show the passage time distribution $W(t)$ corresponding to the line shape function $p_2(\nu)$; the label on each curve gives the dephasing time T_2^*. The dashed curve corresponds to the Gaussian line shape $p_\infty(\nu)$ with $T_2^*=6.75$. Note the difference of this latter curve from the lowest one of the solid curves which refers to the same value of T_2^*. All curves were obtained for $N=1.5\times10^8$, $1/v=0.3$, $I_{ref}=0.03$.

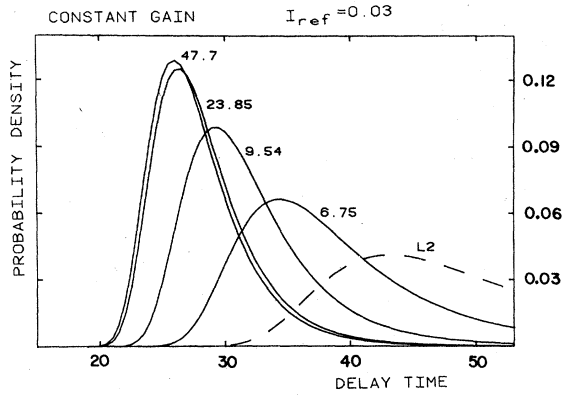

FIG. 6. Same as Fig. 5, except that the solid curves refer to the Gaussian line $p_\infty(\nu)$, and the dashed one to the line shape function $p_2(\nu)$.

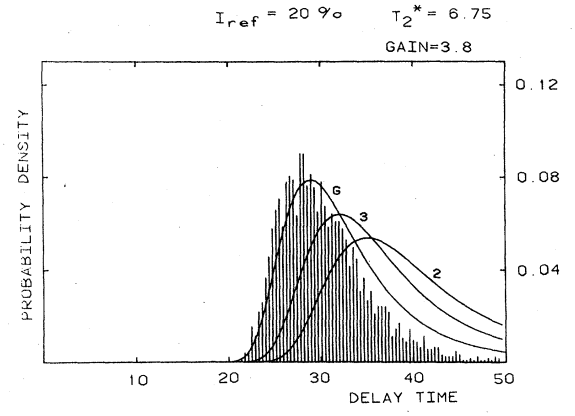

FIG. 7. The histogram gives the passage time distribution as obtained from a large number of numerical solutions of the nonlinear Maxwell-Bloch equations (2.17) (see text). The curves labeled G, 3, and 2 show the result (3.18) for the line shape functions p_∞, p_3, and p_2, respectively.

shown in Fig. 7 are all calculated for identical values of N, v, and T_2^*. The slight shift of the histogram to the left of the distribution $W(t)$ based on the Gaussian line is due to the representation of the atomic line by as few as five frequencies; such a truncated spectrum has, of course, even less weight in its wings than a Gaussian spectrum.

ACKNOWLEDGMENTS

This project was supported in part by a Nato Research Grant, No. 1445, and by the U.S. Department of Energy under Contract No. EY76-C-02-3064.

APPENDIX

In order to evaluate the functional integral (3.14) we begin by regarding it as the limit of a form in which the spatial variable is rendered discrete, $x \to \{x_i\}$,

$$D(\omega,\Omega) \equiv \mathfrak{N} \int \left(\prod_i d^2R_i\right) \exp\left(-\sum_{ij} M_{ij} R_i R_j^*\right),$$

in which

$$M_{ij} \equiv \frac{N}{4}\Delta x \delta_{ij} + (\Delta x)^2[i\omega e_i e_j^* + i\Omega(\dot{e}_j e_j^* + e_i \dot{e}_j^*)] . \tag{A1}$$

To simplify the notation we omit, for the moment, the depencence of R on the frequency ν. Since the normalization condition for the probability distribution (2.25) reads

$$D(0,0) = 1 , \tag{A2}$$

the quantity $D(\omega,\Omega)$ can be written as the ratio of two multiple Gaussian integrals. As is well known, the latter integrals can be expressed in terms of the determinant of the matrix M,

$$D(\omega,\Omega) = \frac{\mathrm{Det}M(0,0)}{\mathrm{Det}M(\omega,\Omega)} = \frac{1}{\mathrm{Det}[M(\omega,\Omega)M(0,0)^{-1}]} = \exp\{-\mathrm{tr}\ \ln[M(\omega,\Omega)M(0,0)^{-1}]\}, \tag{A3}$$

with

$$M(\omega,\Omega)M(0,0)^{-1} = \delta_{ij} + \left(\frac{4\Delta x}{N}\right)[i\omega e_i e_j^* + i\Omega(\dot{e}_i e_j^* + e_i \dot{e}_j^*)] \equiv \delta_{ij} + m_{ij} . \tag{A4}$$

We represent the logarithm of the matrix (A4) by its Taylor series,

$$\ln(1+m) = \sum_{n=1}^{\infty} \frac{(-1)^{n+1}}{n}(m)^n , \tag{A5}$$

and thus find

$$D(\omega,\Omega) = \exp\left(-\sum_n \frac{(-1)^{n+1}}{n}\mathrm{tr}m^n\right) . \tag{A6}$$

The nth power of the matrix m is easily constructed since it obviously has the structure

$$(m^n)_{ij} = e_i e_j^* A_n + e_i \dot{e}_j^* B_n + \dot{e}_i e_j^* C_n + \dot{e}_i \dot{e}_j^* D_n \tag{A7}$$

in which the four coefficients A_n, B_n, C_n, and D_n remain to be determined. These coefficients obey the "initial" conditions

$$A_1 = i\omega(4\Delta x/N), \quad B_1 = C_1 = i\Omega(4\Delta x/N), \quad D_1 = 0$$

and a set of recursion relations which can be written with the help of a suitably defined 2×2 transfer matrix T as

$$\begin{pmatrix} A_{n+1} \\ B_{n+1} \end{pmatrix} = T\begin{pmatrix} A_n \\ B_n \end{pmatrix}, \quad \begin{pmatrix} C_{n+1} \\ D_{n+1} \end{pmatrix} = T\begin{pmatrix} C_n \\ D_n \end{pmatrix}. \tag{A8}$$

The transfer matrix can be expressed in terms of the sums $\sum_i (4\Delta x/N)|e_i|^2$, $\sum_i (4\Delta x/N)|\dot{e}_i|^2$, and $\sum_i (4\Delta x/N)\dot{e}_i e_j^*$. By inverting to the continuum description of the spatial variable x and reinstating the frequency ν as a summation variable, we recognize these sums as the mean values $I = \langle|E|^2\rangle$, $\langle|\dot{E}|^2\rangle$, and $\langle \dot{E}E^*\rangle$, respectively. The definition of the transfer matrix can then be given as

$$T = \begin{pmatrix} i\omega I + i\Omega\langle \dot{E}E^*\rangle & i\omega\langle E\dot{E}^*\rangle + i\Omega\langle|\dot{E}|^2\rangle \\ i\Omega I & i\Omega\langle E\dot{E}^*\rangle \end{pmatrix}. \tag{A9}$$

By noting that the recursion relations (A8) are solved by

$$\begin{pmatrix} A_n \\ B_n \end{pmatrix} = \frac{4\Delta x}{N} T^{n-1}\begin{pmatrix} i\omega \\ i\Omega \end{pmatrix}, \quad \begin{pmatrix} C_n \\ D_n \end{pmatrix} = \frac{4\Delta x}{N} T^{n-1}\begin{pmatrix} i\Omega \\ 0 \end{pmatrix}, \tag{A10}$$

we can, in effect, reduce the problem of finding the trace of the $\infty\times\infty$ matrix m^n to that of a 2×2 matrix. To accomplish that reduction we perform the trace operation in Eq. (A7),

$$\mathrm{tr}m^n = \sum_i (|e_i|^2 A_n + e_i \dot{e}_i^* B_n + \dot{e}_i e_i^* C_n + |\dot{e}_i|^2 C_n), \tag{A11}$$

and insert the result (A10),

$$\begin{aligned} \mathrm{tr}m^n &= (T^{n-1})_{11}(i\omega I + i\Omega\langle \dot{E}E^*\rangle) + (T^{n-1})_{12}(i\Omega I) \\ &\quad + (T^{n-1})_{21}(i\omega\langle E\dot{E}^*\rangle + i\Omega\langle|\dot{E}|^2\rangle) \\ &\quad + (T^{n-1})_{22}(i\Omega\langle E\dot{E}^*\rangle) \\ &= (T^n)_{11} + (T^n)_{22} = \mathrm{tr}T^n . \end{aligned} \tag{A12}$$

The trace of the 2×2 matrix T^n can be expressed in terms of the two eigenvalues $t_\pm$ of the transfer matrix T as

$$\mathrm{tr}m^n = \mathrm{tr}T^n = t_+^n + t_-^n . \tag{A13}$$

We insert this result in the Taylor series (A5) and obtain

$$\mathrm{tr}\ln(1+m)=\ln(1+t_+)+\ln(1+t_-)\ . \tag{A14}$$

The functional integral (A6) is thus

$$D(\omega,\Omega)=\frac{1}{(1+t_+)(1+t_-)}\ . \tag{A15}$$

The two eigenvalues $t_\pm$ of T are easily found. By introducing the function Δ defined in Eq. (3.10), we can write them as

$$t_\pm=\tfrac{1}{2}(i\omega I+i\Omega\dot{I})\pm[\tfrac{1}{4}(i\omega I+i\Omega\dot{I})^2-\Omega^2\Delta^2]^{1/2}\ . \tag{A16}$$

The final result for the functional integral thus takes the simple form

$$D(\omega,\Omega)=(1+i\omega I+i\Omega\dot{I}+\Omega^2\Delta^2)^{-1}\ . \tag{A17}$$

---

[1]Q. H. F. Vrehen, in *Laser Spectroscopy IV*, edited by H. Walther and K. W. Rothe (Springer, Berlin, 1979).

[2]F. Haake, H. King, G. Schröder, J. W. Haus, and R. Glauber, Phys. Rev. A 20, 2017 (1979); F. Haake, H. King, G. Schröder, J. W. Haus, R. Glauber, and F. Hopf, Phys. Rev. Lett. 42, 1740 (1979).

[3]F. Haake, J. W. Haus, H. King, G. Schröder, and R. Glauber, Phys. Rev. Lett. 45, 558 (1980); J. Opt. Soc. Am. 70, 611 (1980).

[4]For a sharp atomic line the early-stage linear theory has also been used in Ref. 5 to calculate normally ordered correlation functions of the electric field and in Refs. 6 and 7 to discuss the delay statistics.

[5]R. Glauber and F. Haake, Phys. Lett. 68A, 29 (1978).

[6]D. Polder, M. F. H. Schuurmans, and Q. H. F. Vrehen, J. Opt. Soc. Am. 68, 699 (1978); Phys. Rev. A 19, 1192 (1979).

[7]M. Gross, unpublished thesis, Ecole Normale Supérieure, Paris, 1980.

[8]W. Heitler, *The Quantum Theory of Radiation* (Oxford University Press, New York, 1954).

[9]The closely related first-passage-time problem is treated, e.g., in *Selected Papers on Noise and Stochastic Processes*, edited by N. Wax (Dover, New York, 1954), see especially, the papers by S. O. Rice and M. Kac therein; see also, A. J. F. Siegert, Phys. Rev. 81, 617 (1951); and D. A. Darling and A. J. F. Siegert, Ann. Math. Stat. 24, 624 (1953).

[10]For the higher transcendental functions erf x, erfc x, $I_m(x)$ occurring in this paper we use the definitions given in M. Abramowitz and I. Stegun, *Handbook of Mathematical Functions* (Dover, New York, 1970).

[11]M. F. H. Schuurmans and D. Polder, Phys. Lett. 72A, 306 (1979); M. F. H. Schuurmans, J. Opt. Soc. Am. 70, 609 (1980).

[12]F. Hopf, P. Meystre, and D. W. McLaughlin, Phys. Rev. A 13, 777 (1976).

[13]In Refs. 6 and 7 the delay statistics are discussed, for a sharp atomic line, by using assumptions equivalent to restricting the initial polarization to be spatially homogeneous. Such a restriction completely disregards the initial independence of the excited atoms. The resulting delay time distribution peaks at appreciably later times than our $W(t)$ given in (3.18), if the same reference intensity is used. The shapes of the distributions do not differ strongly though.

[14]The tendency of the delay time to increase as the dephasing time T_2^* becomes smaller has been noted earlier, see e.g., J. H. Eberly, Nuovo Cim. Lett. 1, 183 (1971); G. S. Agarwal, Phys. Rev. A 4, 1791 (1971); C. R. Friedberg and S. R. Hartmann, Phys. Lett. A38, 227 (1972); E. Ressayre and A. Tallet, Phys. Rev. 30, 1239 (1973); R. Jodoin and L. Mandel, Phys. Rev. A 9, 873 (1974); R. Bonifacio and L. A. Lugiato, *ibid.* 11, 1507 (1975); 12, 587 (1975); J. C. Mac Gillivray and M. S. Feld, *ibid.* 14, 1169 (1975).